Published in final edited form as:
Curr Biol. 2012 April 10; 22(7): 596–600. doi:10.1016/j.cub.2012.02.043.

Wld^S prevents axon degeneration through increased mitochondrial flux and enhanced mitochondrial Ca^{2+} buffering

Michelle A. Avery[1], **Timothy M. Rooney**[1], **Jignesh D. Pandya**[3], **Thomas M. Wishart**[2], **Thomas H. Gillingwater**[2], **James W. Geddes**[3], **Patrick Sullivan**[3], and **Marc R. Freeman**[1,*,#]

[1]Department of Neurobiology, University of Massachusetts Medical School

[2]Euan MacDonald Centre for Motor Neurone Disease Research & Centre for Integrative Physiology, University of Edinburgh, Edinburgh, EH8 9XD, United Kingdom

[3]Spinal Cord and Brain Injury Research Center, Department of Anatomy and Neurobiology, University of Kentucky, Lexington, KY 40536-0509, USA

Summary

Wld^S (slow Wallerian degeneration) is a remarkable protein that can suppress Wallerian degeneration of axons and synapses [1] but how it exerts this effect remains unclear [2]. Here, using *Drosophila* and mouse models, we identify mitochondria as a key site of action for Wld^S neuroprotective function. Targeting the NAD^+ biosynthetic enzyme Nmnat to mitochondria was sufficient to fully phenocopy Wld^S, and Wld^S was specifically localized to mitochondria in synaptic preparations from mouse brain. Axotomy of live wild type axons induced a dramatic spike in axoplasmic Ca^{2+} and termination of mitochondrial movement—Wld^S potently suppressed both of these events. Surprisingly, Wld^S also promoted increased basal mitochondrial motility in axons before injury, and genetically suppressing mitochondrial motility *in vivo* dramatically reduced the protective effect of Wld^S. Intriguingly, purified mitochondria from *Wld^S* mice exhibited enhanced Ca^{2+} buffering capacity. We propose that the enhanced Ca^{2+} buffering capacity of Wld^{S+} mitochondria leads to increased mitochondrial motility, suppression of axotomy-induced Ca^{2+} elevation in axons, and thereby suppression of Wallerian degeneration.

Results and Discussion

Mitochondria as a key site of Wld^S neuroprotective function

Remarkably, the distal fragments of severed axons survive for weeks after axotomy in the *Wld^S* mouse [3–6]. The *Wld^S* mutation resulted from the fusion of two neighboring genes and lead to the production of a novel hybrid protein (Wld^S) composed of the 70 NH-terminal amino acids of the E4 ubiqutin ligase Ube4b, a novel 18 amino acid linker domain, and the

[#]Correspondence to marc.freeman@umassmed.edu.
[*]Howard Hughes Medical Institute, Worcester, MA 01605-2324, USA

NAD^+ biosynthetic enzyme Nmnat1 [7]. We previously found that expression of mouse Nmnat3 in *Drosophila* olfactory receptor neuron (ORN) axons provided protection equivalent to Wld^S 5 days after axotomy [8]. Recent work has shown that Nmnat3 expression in mouse neurons also robustly protects axons [9]. We co-expressed mouse *UAS-Nmnat3::Myc* and the mitochondrial marker *UAS-mito::GFP* in *Drosophila* ORNs. We found Nmnat3::Myc localized in a punctate pattern in ORN axons that precisely overlapped with mito::GFP (Figure 1A), indicating that Nmnat3 localized predominantly, if not exclusively, to mitochondria. We next assayed ORN axon preservation at 10, 20, and 50 days after axotomy. We found that Nmnat3 protected axons at levels indistinguishable from Wld^S at all time points tested (Figure 1B). Thus the N70 and W18 domains of Wld^S are dispensable for axon protection if Nmnat activity is targeted to mitochondria. By contrast, expression of Nmnat2 in ORN axons failed to suppress Wallerian degeneration, despite the fact that Nmnat2::Myc was localized throughout the axonal compartment (Supplementary Figure 1A).

Recently *Yahata et al.* (9) reported that in mouse neurons Wld^S protein is located in mitochondria, cytosol, perosixome/lysosome, and ER/Golgi-enriched cell fractions. We revisited Wld^s localization in isolated mouse striatum from control and Wld^s mice by separating the tissues into 3 fractions: non-synaptic striatal tissue, striatal synaptosomes without mitochondria, and synaptic mitochondria. We found Wld^S was detectable in the non-synaptic fraction, as would be expected from its predominantly nuclear localization. In addition, we detected Wld^S in synaptic mitochondria, but not in mitochondria-free synaptic preparations (Supplementary Figure 1B). These data are consistent with a primarily mitochondrial localization of Wld^S in axons and synapses *in vivo* in mouse brain.

Wld^S suppresses termination of mitochondrial motility after injury and axotomy-induced increases in axonal Ca^{2+}

We assayed mitochondrial dynamics in live *Drosophila* axons using the *Tdc2-Gal4* driver, which is expressed in only 3 axons per segment of larval peripheral nerve, by driving *UAS-mCD8::mCherry* (to label axonal membranes) and *UAS-mito::GFP* (to label mitochondria; Figure 3A). In uninjured axons we found no differences in the total number of mitochondria, mitochondrial morphology, or mitochondrial size when we compared control and Wld^S-expressing axons (Supplementary Figure 1A,B). In control animals we found ~35% of mitochondria were motile before injury, but all motility terminated after laser axotomy (Supplementary Movie 1). In striking contrast, we found that laser axotomy of Wld^S-expressing axons had no effect on mitochondrial movement (Supplementary Movie 2; Figure 1C).

Axon injury in mammals leads to extracellular Ca^{2+} entry, which is necessary and sufficient for Wallerian degeneration [10]. Mitochondrial motility is known to be potently modulated by Ca^{2+} [11, 12]. We therefore sought to determine whether *Drosophila* axons showed axotomy-induced changes in axonal Ca^{2+}, and whether axonal Ca^{2+} signaling was modulated by Wld^S. We drove the expression of the genetically-encoded Ca^{2+} indicator GCaMP3 in axons and measured changes in GCaMP3 signals in distal axon segments after laser-induced axotomy. In control animals we found a rapid increase in Ca^{2+} levels within

seconds after axotomy, with Ca^{2+} levels peaking within 1 minute after cut, and then returning towards baseline levels over the next hour (Figure 2A,B,C; Supplementary Movie 3). However, >1 hour after axotomy axonal Ca^{2+} levels remained significantly elevated above baseline (~20% increase). Strikingly, while baseline Ca^{2+} levels in Wld^{S+} axons were indistinguishable from those in controls (Supplementary Figure 3C), in Wld^{s+} axons injury-induced Ca^{2+} bursts were almost completely eliminated: Ca^{2+} levels only rose to ~15% control levels and returned to baseline within 1.5 minutes (Figure 2C; Supplementary Movie 4).

In previous work we generated a collection of *UAS*-regulated Wld^{s}-derived molecules that suppress Wallerian degeneration to varying degrees [8] (Supplementary Figure 1C). We assayed axotomy-induced changes in GCaMP3 fluorescence in axons expressing each of these molecules in live larval preparations. As with Wld^{s}, we found no evidence for changes in axonal mitochondrial number, morphology, or size in these backgrounds (Supplementary Figure 2A,B). However, we found a striking correlation between axon protective function and suppression of axotomy-induced increases in axonal Ca^{2+}: Wld^{s} and Nmnat3 strongly suppressed Wallerian degeneration and post-injury axonal Ca^{2+} increases; Nmnat1, ΔN16::Wld^{s}, and $Wld^{s\text{-}dead}$ partially suppressed Wallerian degeneration and post-injury axonal Ca^{2+} increases; and $Nmant1^{dead}$, which lacks NAD^{+} biosynthetic activity and provided no protection from Wallerian degeneration [8], did not affect post-injury axonal Ca^{2+} increases. These changes were evident in both the distal and proximal axon segment, and affected both peak axonal Ca^{2+} intensities and recovery times to baseline Ca^{2+} levels (Figure 2C,D,E; Supplementary Figures 3A,B).

Wld^{S} enhances mitochondrial movement, which is essential for maximal axonal protection after injury

Since mitochondrial motility is Ca^{2+}-modulated we reasoned that changes in axonal Ca^{2+} buffering might affect axonal mitochondrial motility. We therefore assayed mitochondrial flux in axons expressing Wld^{S}-derived neuroprotective molecules. Surprisingly, we found a significant change in basal mitochondrial motility: in control animals ~35% of total axonal mitochondria were motile, however ~65% of mitochondria were motile in Wld^{s+} axons. Moreover, we found that molecules that provide partial suppression of Wallerian degeneration (Nmnat1, ΔN16::Wld^{S}, and $Wld^{S\text{-}dead}$) led to a modest, but significant, increase in the number of motile mitochondria, while molecules that maximally suppress Wallerian degeneration (Wld^{S}, N16::Nmnat1, and Nmnat3) led to a robust increase in the number of motile mitochondria (Figure 3B). This change in mitochondrial flux in Wld^{S} axons appears to represent a decrease in docked mitochondria, an increase in motile mitochondria, but no significant change in pause/release rates for individual mitochondria (Figure 3C).

Is increased mitochondrial flux critical for Wld^{S}-mediated axon protection? The adapter protein Miro functions to tether mitochondria to cytoskeletal motor proteins and modulate mitochondrial movement in a Ca^{2+}-dependent fashion [12]. Impressively, mutations in *miro* dominantly decrease mitochondrial motility [13]. We therefore crossed strong alleles of *miro* (*miro*^{SD32} and *miro*^{SD26}) and a *UAS*-regulated version of Miro (*UAS-myc::Miro*),

which when overexpressed acts as a dominant negative [13] into the Wld^S background and assayed mitochondrial flux. We found that *miro* mutants or expression of Myc::Miro dominantly suppressed mitochondrial movement in controls. In addition, we found that loss of Miro function also decreased mitochondrial movement in the presence of Wld^S to levels found in control animals (Supplementary Figure 2C,D). Remarkably, reduced *miro* function also dominantly suppressed the neuroprotective effects of Wld^S in ORN axotomy assays. In animals with reduced *miro* function, axon loss was evident by 5 days after axotomy, with synaptic regions showing significant degeneration, and by 30 days after axotomy the protection afforded by Wld^S is almost completely blocked (Figure 3D,E).

Mitochondria from Wld^S-expressing axons show enhanced Ca^{2+} buffering capacity and resistance to formation of the permeability transition pore

Mitochondria are major sinks for cellular Ca^{2+} in both axons and synapses [14]. A powerful mechanism by which Wld^S could exert all of these effects would be by altering mitochondrial Ca^{2+} buffering capacity. We therefore assessed mitochondrial Ca^{2+} cycling/capacity in cortical mitochondria isolated from young (~p25) wild type (NJ) and Wld^S mice. Mitochondrial isolations [15, 16] from both control and *Wld*^{S} animals yielded healthy, well-coupled mitochondria (Figure 4A,B). No apparent difference was observed in the Ca^{2+} uptake rates in mitochondria isolated from Wld^S versus control mice (Figure 4A,B). In contrast, the threshold for mitochondrial permeability, indicated by the loss of membrane potential (Figure 4A) and mitochondrial release of Ca^{2+} (Figure 4B), was significantly greater in mitochondria from Wld^S mice (Figure 4C). Thus, following increases in cytoplasmic Ca^{2+}, Wld^S mitochondria isolated from mouse brain buffer higher loads of Ca^{2+} before releasing it back into the cytoplasmic compartment via the mitochondria permeability transition pore (PTP).

Conclusions

The mechanistic action of Wld^s has remained controversial, but recent work has established a non-nuclear role for Wld^s [2] after injury [17]. In this study we show that Wld^S is localized to mitochondria *in vivo*. It is important to note that protein localization studies with Wld^s must be interpreted cautiously—the primarily nuclear localization of Wld^s suggested a nuclear role for Wld^s and initially misled the field [2]. However, we also find that Wld^s increases mitochondrial Ca^{2+} buffering capacity, and results in maintained mitochondrial motility after axotomy. Taken together, these data argue strongly that the mitochondrial compartment is a key site of action for Wld^S *in vivo*.

We have shown that axonal injury in live *Drosophila* preparations leads to a dramatic and transient rise in axonal Ca^{2+}. Increased axonal Ca^{2+} has been observed in mammals after acute nerve crush [18] and entry of extracellular Ca^{2+} is necessary and sufficient for Wallerian degeneration [10]. Impressively, Wld^s expression resulted in a striking suppression of this axotomy-induced rise in axonal Ca^{2+}. The most plausible explanation for this enhanced buffering is that increased ATP/energy production observed in Wld^{s+} mitochondria [9]—presumably via increased mitochondrial NAD^+ production, though we cannot formally exclude essential roles for other substrates of Nmnat—is linked to increased

mitochondrial membrane potential ($\Delta\psi m$), and thereby increased Ca^{2+} entry through the $\Delta\psi m$–regulated mitochondrial Ca^{2+} uniporter [19]. This model is supported by our observation that Wld^{S}-expressing mitochondria isolated from mouse brain exhibit an enhanced ability to maintain their membrane potential and avoid PTP formation in the face of increasing extramitochondrial Ca^{2+}. In the future it will be important to confirm that such changes are also observed in *Drosophila* axonal mitochondrial physiology *in vivo* in Wld^{S}-expressing neurons.

Axonal Ca^{2+} spikes could result solely from entry of extracellular Ca^{2+} into the axon after injury. This would be consistent with the observation that blocking Ca^{2+} channels inhibits Wallerian degeneration [10, 18]. Mitochondria are a well-established sink for Ca^{2+} in axons [14] and here we show that Wld^{S+} mitochondria exhibit enhanced Ca^{2+} buffering capacity and resistance to Ca^{2+}-induced formation of the permeability transition pore (PTP). Indeed PTP formation appears to be a key final execution step in Wallerian degeneration [20–22]. We therefore favor a model whereby extracellular Ca^{2+} enters the axon after axotomy and normally acts as a switch to activate Wallerian degeneration. In Wld^{S} axons this Ca^{2+} is instead rapidly buffered by mitochondria, thereby blocking induction of axonal destruction. Consistent with this model, uncoupling mitochondria, which suppresses mitochondrial Ca^{2+} uptake [23, 24], completely abrogates the protective effect of Wld^{S} *in vitro* [25].

Wld^{S}-expressing neurons exhibit a roughly 2-fold increase in the number of motile versus stationary mitochondria compared to wild type controls, which could result from changes in mitochondrial Ca^{2+} buffering. Notably, genetic suppression of enhanced mitochondrial flux using mutations in *miro* also resulted in a remarkable suppression of Wld^{S}-mediated axonal protection *in vivo*. However, since this suppression was only partial, additional factors beyond increases in mitochondrial motility must also contribute to Wld^{S}-mediated axonal protection. For example, axonal energy supplies are likely closely intertwined with mitochondrial transport and bioenergetics. Wld^{S+} mitochondria are known to exhibit an enhanced ability to generate ATP [9]. This change in bioenergetics, coupled with increased mitochondrial motility in Wld^{S+} axons might enhance distribution of ATP or other mitochondrially-derived metabolites. At the same time, enhanced mitochondrial motility could also speed the removal of metabolic byproducts normally processed by mitochondria. Similarly, increased mitochondrial motility in axons could further enhance mitochondrial Ca^{2+} buffering in Wld^{S+} axons since motile mitochondria would be predicted to traverse more — axonal space, and perhaps be exposed to more Ca^{2+} than stationary mitochondria. Together these could have the combined effect of increasing energy delivery, removing harmful byproducts, and increased buffering of Ca^{2+}, a signal that can potently activate axonal degeneration.

A role for mitochondria in the Wld^{S} neuroprotective mechanism is intriguing since defects in mitochondria respiration and dynamics are emerging as critical underlying factors in a number of neurological disorders [26]. For example, in mouse models of ALS (SOD1 transgenics) anterograde [27] and retrograde [28] mitochondrial transport is reduced; altered mitochondrial trafficking has been observed in models of Alzheimers disease [29]; and mutant, but not wild type Huntington protein blocks mitochondrial movement in cortical neurons [30]. However, in the majority of models, whether these mitochondrial alterations

are a cause or consequence of disease remains an open question [26]. Our study shows, reciprocally, that enhanced mitochondrial flux is associated with, and is required for maximal axon protection by Wld^S.

Supplementary Material

Refer to Web version on PubMed Central for supplementary material.

Acknowledgments

This work was supported by NIH grant NS062993 (JWG and PGS), the Wellcome Trust (THG and MRF), NIH grant NS059991 (to MRF) and MRF is an Early Career Scientist with the Howard Hughes Medical Institute. TMR was supported by a grant from the DOD (BC093796). We thank Vimala Bondada and Dingyuan Lou for preliminary work on the mitochondrial Ca^{2+} dynamics, and all members of the laboratories for helpful discussions.

References

1. Conforti L, Tarlton A, Mack TG, Mi W, Buckmaster EA, Wagner D, Perry VH, Coleman MP. A Ufd2/D4Cole1e chimeric protein and overexpression of Rbp7 in the slow Wallerian degeneration (WldS) mouse. Proc Natl Acad Sci U S A. 2000; 97:11377–11382. [PubMed: 11027338]
2. Coleman MP, Freeman MR. Wallerian degeneration, wld(s), and nmnat. Annu Rev Neurosci. 2010; 33:245–267. [PubMed: 20345246]
3. Lunn ER, Perry VH, Brown MC, Rosen H, Gordon S. Absence of Wallerian Degeneration does not Hinder Regeneration in Peripheral Nerve. Eur J Neurosci. 1989; 1:27–33. [PubMed: 12106171]
4. Perry VH, Brown MC, Lunn ER, Tree P, Gordon S. Evidence that Very Slow Wallerian Degeneration in C57BL/Ola Mice is an Intrinsic Property of the Peripheral Nerve. Eur J Neurosci. 1990; 2:802–808. [PubMed: 12106282]
5. Glass JD, Brushart TM, George EB, Griffin JW. Prolonged survival of transected nerve fibres in C57BL/Ola mice is an intrinsic characteristic of the axon. J Neurocytol. 1993; 22:311–321. [PubMed: 8315413]
6. Gillingwater TH, Ingham CA, Parry KE, Wright AK, Haley JE, Wishart TM, Arbuthnott GW, Ribchester RR. Delayed synaptic degeneration in the CNS of Wlds mice after cortical lesion. Brain. 2006; 129:1546–1556. [PubMed: 16738060]
7. Mack TG, Reiner M, Beirowski B, Mi W, Emanuelli M, Wagner D, Thomson D, Gillingwater T, Court F, Conforti L, et al. Wallerian degeneration of injured axons and synapses is delayed by a Ube4b/Nmnat chimeric gene. Nat Neurosci. 2001; 4:1199–1206. [PubMed: 11770485]
8. Avery MA, Sheehan AE, Kerr KS, Wang J, Freeman MR. Wld S requires Nmnat1 enzymatic activity and N16-VCP interactions to suppress Wallerian degeneration. J Cell Biol. 2009; 184:501–513. [PubMed: 19237597]
9. Yahata N, Yuasa S, Araki T. Nicotinamide mononucleotide adenylyltransferase expression in mitochondrial matrix delays Wallerian degeneration. J Neurosci. 2009; 29:6276–6284. [PubMed: 19439605]
10. George EB, Glass JD, Griffin JW. Axotomy-induced axonal degeneration is mediated by calcium influx through ion-specific channels. J Neurosci. 1995; 15:6445–6452. [PubMed: 7472407]
11. Yi M, Weaver D, Hajnoczky G. Control of mitochondrial motility and distribution by the calcium signal: a homeostatic circuit. J Cell Biol. 2004; 167:661–672. [PubMed: 15545319]
12. Wang X, Schwarz TL. The mechanism of Ca2+-dependent regulation of kinesin-mediated mitochondrial motility. Cell. 2009; 136:163–174. [PubMed: 19135897]
13. Russo GJ, Louie K, Wellington A, Macleod GT, Hu F, Panchumarthi S, Zinsmaier KE. Drosophila Miro is required for both anterograde and retrograde axonal mitochondrial transport. J Neurosci. 2009; 29:5443–5455. [PubMed: 19403812]
14. Ganitkevich VY. The role of mitochondria in cytoplasmic Ca2+ cycling. Exp Physiol. 2003; 88:91–97. [PubMed: 12525858]

15. Brown MR, Sullivan PG, Dorenbos KA, Modafferi EA, Geddes JW, Steward O. Nitrogen disruption of synaptoneurosomes: an alternative method to isolate brain mitochondria. J Neurosci Methods. 2004; 137:299–303. [PubMed: 15262074]
16. Naga KK, Sullivan PG, Geddes JW. High cyclophilin D content of synaptic mitochondria results in increased vulnerability to permeability transition. J Neurosci. 2007; 27:7469–7475. [PubMed: 17626207]
17. Sasaki Y, Milbrandt J. Axonal degeneration is blocked by nicotinamide mononucleotide adenylyltransferase (Nmnat) protein transduction into transected axons. J Biol Chem. 2010; 285:41211–41215. [PubMed: 21071441]
18. Knoferle J, Koch JC, Ostendorf T, Michel U, Planchamp V, Vutova P, Tonges L, Stadelmann C, Bruck W, Bahr M, et al. Mechanisms of acute axonal degeneration in the optic nerve in vivo. Proc Natl Acad Sci U S A. 2010; 107:6064–6069. [PubMed: 20231460]
19. Santo-Domingo J, Demaurex N. Calcium uptake mechanisms of mitochondria. Biochim Biophys Acta. 2010; 1797:907–912. [PubMed: 20079335]
20. Sievers C, Platt N, Perry VH, Coleman MP, Conforti L. Neurites undergoing Wallerian degeneration show an apoptotic-like process with Annexin V positive staining and loss of mitochondrial membrane potential. Neurosci Res. 2003; 46:161–169. [PubMed: 12767479]
21. Sunio A, Bittner GD. Cyclosporin A retards the wallerian degeneration of peripheral mammalian axons. Exp Neurol. 1997; 146:46–56. [PubMed: 9225737]
22. Barrientos SA, Martinez NW, Yoo S, Jara JS, Zamorano S, Hetz C, Twiss JL, Alvarez J, Court FA. Axonal degeneration is mediated by the mitochondrial permeability transition pore. J Neurosci. 2011; 31:966–978. [PubMed: 21248121]
23. Pandya JD, Pauly JR, Sullivan PG. The optimal dosage and window of opportunity to maintain mitochondrial homeostasis following traumatic brain injury using the uncoupler FCCP. Exp Neurol. 2009; 218:381–389. [PubMed: 19477175]
24. Pandya JD, Pauly JR, Nukala VN, Sebastian AH, Day KM, Korde AS, Maragos WF, Hall ED, Sullivan PG. Post-Injury Administration of Mitochondrial Uncouplers Increases Tissue Sparing and Improves Behavioral Outcome following Traumatic Brain Injury in Rodents. J Neurotrauma. 2007; 24:798–811. [PubMed: 17518535]
25. Ikegami K, Koike T. Non-apoptotic neurite degeneration in apoptotic neuronal death: pivotal role of mitochondrial function in neurites. Neuroscience. 2003; 122:617–626. [PubMed: 14622905]
26. Schon EA, Przedborski S. Mitochondria: the next (neurode)generation. Neuron. 2011; 70:1033–1053. [PubMed: 21689593]
27. De Vos KJ, Chapman AL, Tennant ME, Manser C, Tudor EL, Lau KF, Brownlees J, Ackerley S, Shaw PJ, McLoughlin DM, et al. Familial amyotrophic lateral sclerosis-linked SOD1 mutants perturb fast axonal transport to reduce axonal mitochondria content. Hum Mol Genet. 2007; 16:2720–2728. [PubMed: 17725983]
28. Shi P, Strom AL, Gal J, Zhu H. Effects of ALS-related SOD1 mutants on dynein- and KIF5-mediated retrograde and anterograde axonal transport. Biochim Biophys Acta. 2010; 1802:707–716. [PubMed: 20510358]
29. Wang X, Su B, Zheng L, Perry G, Smith MA, Zhu X. The role of abnormal mitochondrial dynamics in the pathogenesis of Alzheimer's disease. J Neurochem. 2009; 109(Suppl 1):153–159. [PubMed: 19393022]
30. Chang DT, Rintoul GL, Pandipati S, Reynolds IJ. Mutant huntingtin aggregates impair mitochondrial movement and trafficking in cortical neurons. Neurobiol Dis. 2006; 22:388–400. [PubMed: 16473015]

Highlights

- Axotomy induces dramatic Ca^{2+} bursts and termination of mitochondrial motility in axons
- Wld^S suppresses axotomy-induced Ca^{2+} bursts and axons maintain mitochondrial motility after axotomy
- Wld^S is localized to mitochondria and enhances mitochondrial Ca^{2+} buffering, resistance to mPTP, and mitochondrial motility *in vivo*
- Enhanced mitochondrial motility is essential for Wld^S neuroprotective function

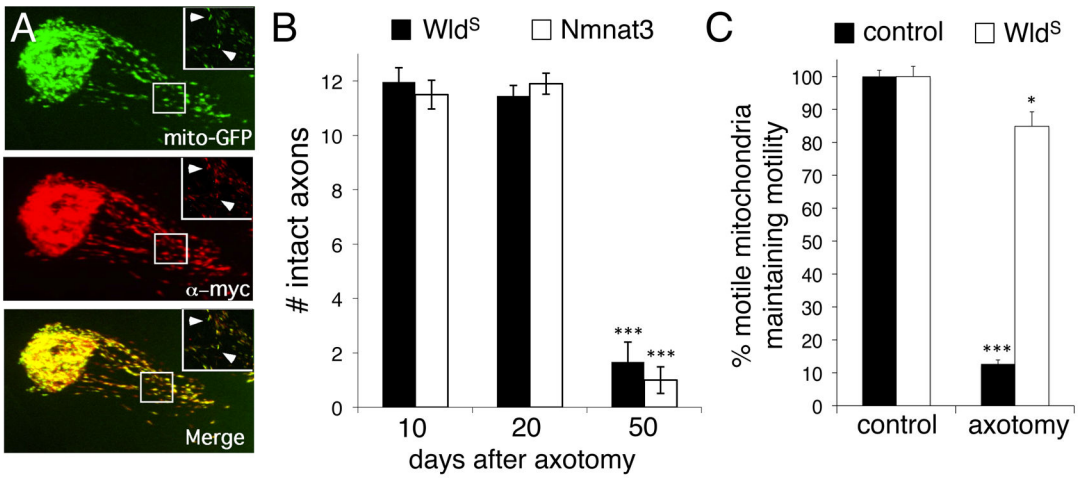

Figure 1. Mitochondria as a focal point for Wld^S-mediated axon protection

(A) Mouse Nmnat3::Myc localizes to mitochondria in *Drosophila* axons. *22a-Gal4* was used to drive *UAS-Nmnat3::Myc* and *UAS-mito::GFP*. Insets show boxed region.

(B) Mitochondrial Nmnat3 fully mimics Wld^S in axon protective function. *22a-Gal4* was used to drive *UAS-Nmnat3* or *UAS-Wld^S* in a background where axons were labeled with membrane-tethered GFP (*UAS-mCD8::GFP*). n≥20 antennal lobes for each. *** indicates p<0.001. Error bars represent ±SEM.

(C) Wld^S-suppresses axotomy-induced termination of mitochondrial motility. Mitochondrial movement was assessed in live open-filet preparations of third instar *Drosophila* larvae immediately after axotomy for 5 minutes. Axotomy was induced by severing axons with a Micropoint laser ablation system and confirmed by a breakage of mCD8::mCherry-labeled axons. n≥10 live samples for each genotype and time point. ***, p<0.001.

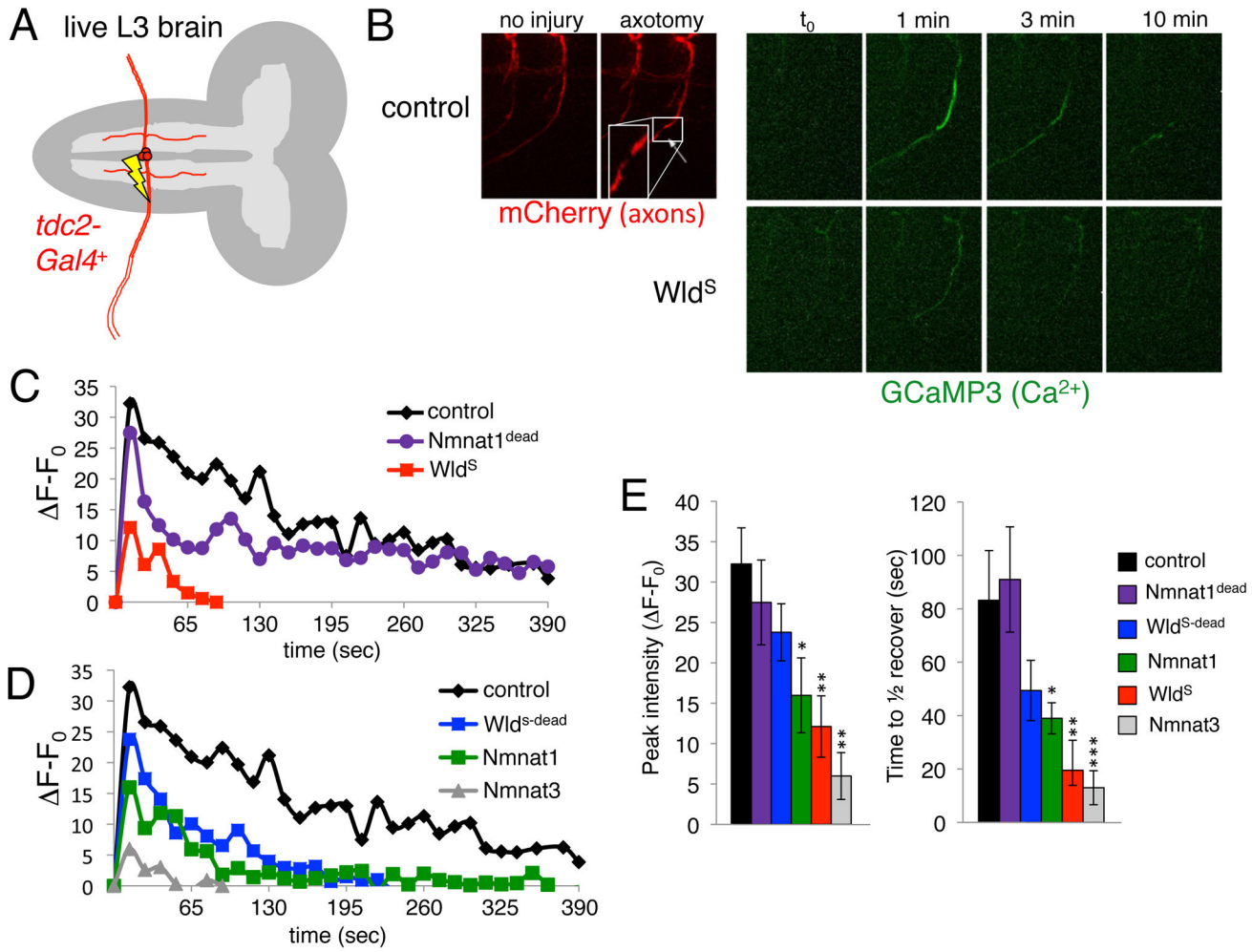

Figure 2. *In vivo* laser axotomy induces a dramatic rise in axonal Ca^{2+} that is suppressed by Wld^S

(A) *tdc2-Gal4* labels 3 axons in each peripheral nerve, only one segment is illustrated.

(B) Axons were labeled with mCD8::mCherry, axonal Ca^{2+} was monitored by co-expressing GCaMP3 in the *tdc2-Gal4*$^+$ subset of neurons. Note the breakage of the axon after laser axotomy (red, mCherry). Axonal Ca^{2+} levels one minute after axotomy (green, GCaMP3).

(C,D) Representative traces showing Ca^{2+} responses in axon fragments distal to the injury site over time. Genotypes as indicated.

(E) Quantification of peak Ca^{2+} intensities and time to ½ recovery from average peak intensity for each genotype listed. n≥5 live samples for each genotype and time point versus control. *, p<0.05; **, p<0.01; ***, p<0.001.

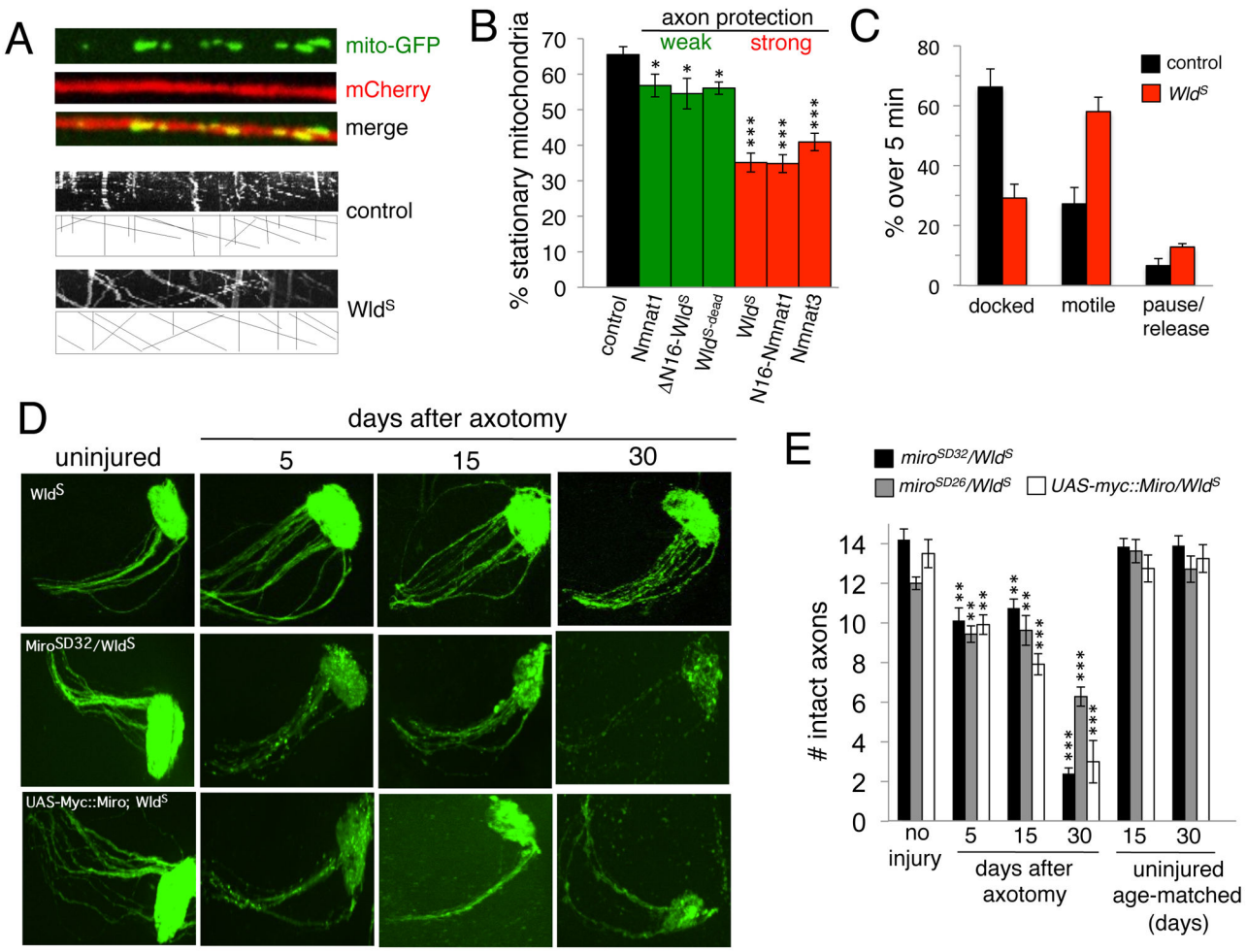

Figure 3. Wld^S increases mitochondrial flux, which is essential for neuroprotective function

(A) Mitochondrial flux was assayed in *tdc2-Gal4*-expressing neurons in live preparations of third instar larvae. Representative kymographs of mitochondrial movement are shown for control and Wld^S-expressing axons. Anterograde is to the right, retrograde is to the left.

(B) Mitochondrial flux was assayed in axons expressing each of the following molecules: Nmnat1, DN16-Wld^S, Wld$^{S\text{-dead}}$, Wld^S, N16-Nmnat1, and Nmant3. n≥10 live samples for each genotype. *, p<0.05; ***, p<0.001.

(C) Quantification of the movement of individual mitochondrial by binning into mobile, docked, or pausing/releasing during a 5 minute window. n=5 movies for each genotype.

(D) ORN axotomy assays in Wld^S backgrounds and *miro* mutants. A single antennal lobe where ORN axons were severed is shown.

(E) Quantification of data from (D). Age-matched uninjured controls at the same time points are shown at right. n≥15 samples for each genotype and time point. **, p<0.01; ***, p<0.001.

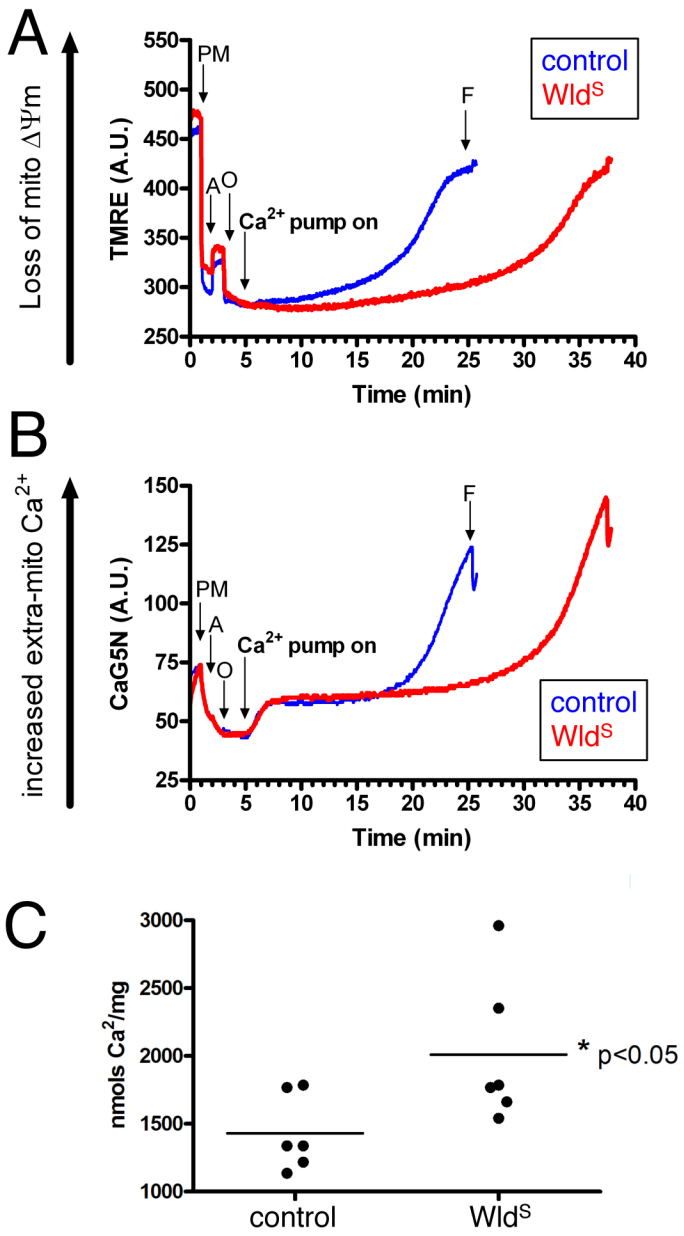

Figure 4. Wld^S brain mitochondria display higher Ca^{2+} load capacity than age matched wild type (NJ) controls

(A,B) TMRE (membrane potential indicator) and CaG5N (extra-mitochondrial Ca^{2+} indicator) fluorescence were monitored over time simultaneously for each sample of non-synaptic mitochondria. As illustrated in TMRE traces for the first three minutes, the addition of pyruvate and malate (PM) an oxidative substrate, causes a marked downward deflection at 1 minute due to increased mitochondrial membrane potential (Δψm). Following ADP (A) addition, the loss of Δψm is indicated by upward deflection at 2 mins as Δψm is utilized to phosphorylate ADP to ATP via proton flow thru the ATP synthase. The ATP synthase inhibitor, oligomycin (O) addition at 3 min results in maximum Δψm as proton flow is inhibited. The Ca^{2+} infusion began at 5 min (infusion rate 160 nmol of Ca^{2+}/mg protein/

min) and was monitored by CaG5N fluorescence, and is illustrated by the initial upward deflection followed by constant signal due to mitochondrial Ca^{2+} uptake into the matrix. The subsequent rise in CaG5N fluorescence accompanied by a loss of membrane potential signifies mitochondrial permeability transition and subsequent release of mitochondrial Ca^{2+}.

(C) Quantification of mitochondrial Ca^{2+} buffering capacity (nmols/mg protein) indicates that Wld^S non-synaptic mitochondria sequestered significantly higher amounts of Ca^{2+} compared to control group (n=6/group, * $p<0.05$, unpaired t-test).